Control of the adsorption properties of alginate - guar gum matrix functionalized with epichlorohydrin through the addition of different flexible chain polymers as toll for the chymotrypsinogen isolation

M. Emilia Brassesco, Nadia Woitovich Valetti, Guillermo A. Picó

PII: S0141-8130(17)35106-1
DOI: doi:10.1016/j.ijbiomac.2018.04.087
Reference: BIOMAC 9495

To appear in:

Received date: 20 December 2017
Accepted date: 16 April 2018

Please cite this article as: M. Emilia Brassesco, Nadia Woitovich Valetti, Guillermo A. Picó , Control of the adsorption properties of alginate - guar gum matrix functionalized with epichlorohydrin through the addition of different flexible chain polymers as toll for the chymotrypsinogen isolation. The address for the corresponding author was captured as affiliation for all authors. Please check if appropriate. Biomac(2017), doi:10.1016/j.ijbiomac.2018.04.087

Control of the adsorption properties of alginate - guar gum matrix functionalized with Epichlorohydrin through the addition of different flexible chain polymers as toll for the chymotrypsinogen isolation

M. Emilia Brassesco, Nadia Woitovich Valetti and Guillermo A. Picó

Institute of Biotechnological and Chemistry Processes. Faculty of Biochemical and Pharmaceutical Sciences and CONICET. National University of Rosario. Suipacha 570 (S2002RLK) Rosario. Argentina

Keywords: alginate; guar gum; polyelectrolytes; chymotrypsinogen; adsorption; isotherms

Abbreviations: GG; guar gum, Alg; alginate, QTg; chymotrypsinogen, PVA; polyvinyl alcohol, PVP; polyvinyl pyrrolidine, FCP; flexible chain polymer, P68; Pluronic F68.

Send correspondence to:
Dr. Guillermo A. Picó
Institute of Biotechnological and Chemistry Processes
Faculty of Biochemical and Pharmaceutical Sciences
Nacional University of Rosario
Suipacha 570
(S2002RLK) Rosario
FAX +54(0341) 480 4598
ARGENTINA
e-mail: pico@iprobyq-conicet.gob.ar

Abstract

This work addresses the obtaining and characterization of alginate-guar gum matrix, cross-linked with epichlorohydrin in the presence of different flexible chain polymers: polyvinyl alcohol, polyvinyl pyrrolidine and Pluronic® F68. These matrixes were used for the adsorption of chymotrypsinogen and showed an increasing uptake in presence of the flexible chain polymer in the sense: none < Pluronic 68 < polyvinyl pyrrolidine < polyvinyl alcohol. The adsorption process was found to follow a first order kinetics model and was not influenced by the polymer type. It was found that Freundlich model was more suitable for our data. Polyvinyl alcohol and polyvinyl pyrrolidine addition increase the adsorption capacity of the original bed due to an increment in the rigidity of the gel caused by the formation of hydrogen bound between the polysaccharides and synthetics polymers.

Highlights

. Alginate-guar gum bed adsorbs chymotrypsinogen.

. The adsorption process fitted a Freundlich isotherm.

. The presence of polyvinyl alcohol increases the protein adsorption- desorption process.

. The bed remained functional until the tenth cycle of repeated batch enzyme adsorption.

1. Introduction

Trypsin and chymotrypsin are serine proteases produced by the pancreas in a non-active form: trypsinogen and chymotrypsinogen (QTg), respectively [1]. These enzymes are widely used in different biotechnological industries such as food, pharmaceutical, etc. However, despite the great use of these enzymes, their only sources are bovine or porcine pancreas, because microorganisms have a very low yield expression of these enzymes. From the classical work of Northrop and Kunitz [2] on the isolation and characterization of the pancreatic zymogens, different methods have been proposed for obtaining them from fresh bovine pancreas. The general way to isolate these enzymes is submerging the freshly collected pancreas in 0.25 N sulfuric acid, then, making a homogenate and finally, the zymogens are recovered by fractional precipitation with ammonium sulfate (50 to 70 % of saturation). Besides, ionic exchange chromatography is used to separate the QTg from trypsinogen [2, 3]. Other method induces previously the activation of the zymogen and the activated proteases are isolated by ionic exchange chromatography with a salt gradient [4]. In previous reports we have analyzed the possibility to isolate bovine proteases from pancreas using precipitation of the active enzymes by complex formation with synthetic and natural polyelectrolytes [5, 6], however, the yield of the process is low due to the loss of active enzyme by self-destruction.

Solute adsorption onto a bed in batch or on a packed bed is a powerful way to isolate, concentrate and purify proteins at a scaling up level. The successful application of adsorption process requires the matrix to be chemically and physically stable, with high mechanical strength or resistance to breakage, easily penetrable by solute, easy of handle, and economically competitive. Commercial matrixes are expensive especially if they are used in large-scale methods. So, the development of a new economic matrix,

easy to prepare in great amount is required in the downstream processing of industrial enzymes. The use of natural polymers such as polysaccharides to obtain matrixes with capacity to adsorb proteins is an excellent option, because they are easy to prepare in great scale, profitable and they can be discarded in the environment without any negative impact. A variety of polysaccharides having net electrical charge have been used such like: alginate (Alg), chitosan, pectin, carrageenan, etc. [7-9]. To increase the penetrability of these matrixes a second non-charged polysaccharide is added. However, when these matrixes are used for the adsorption of a target molecule from its natural biomass, the latter induced an interference in the adsorption process, resulting in a low capacity of adsorption of target molecule. Another improvement that is intended is the addition to the bed of a non-ionic flexible chain polymer (FCP) that avoids the interaction with the biomass increasing the yield of the extraction process. Such is the case of Pluronic® F68 (P68), polyvinyl pyrrolidine (PVP) and polyvinyl alcohol (PVA), which modifies the structure of the bed, inducing a higher degree of interaction between it and the protein, increasing the mechanical stability and the recycling of the bed. Lahorde et al. [10, 11] demonstrated that the addition of a flexible chain polymer (FCP) to a commercial bed as Streamline® induced a minor interaction of the biomass with the bed, favoring the capture of the target macromolecule by the matrix. Also, the presence of a hydrophobic-hydrophilic flexible chain polymer inside the bed increased the capacity to adsorb proteins and the stability of the adsorbed enzyme.

In this work, we obtained a bed formed by Alg and guar gum (GG), cross-linked with epichlorohydrin in the presence of different FCP and we studied the influence of these FCPs on the adsorption of QTg onto the bed, determining the molecular mechanism by which this process is carried out. The objective of these studies is given in the

possibility of obtaining matrix with greater capacity of adsorption, mechanically more resistant, with little interaction with the biomass and low cost.

2. Materials and methods

2.1. Chemical: Alginic acid sodium salt (Alg), guar gum (GG), epichlorohydrin, polyvinyl pyrrolidine (PVP), Pluronic F68® (P68), polyvinyl alcohol (PVA) and chymotrypsinogen (QTg) were purchased from Sigma-Aldrich and used without further purification. All other reagents were also of analytical grade. The solutions were prepared with distilled water.

2.2. Preparation of Alg–GG beads: Beads were formed by dropping polymer solution through a syringe into 0.1M $CaCl_2$ solution according to the method previously reported by Roy et al. [12]. The cross-linked process was carried out following the protocol used in a previous work [13]. Four matrixes were prepared: Alg-GG with the final concentration of 0.6 %P/V: 0.5 %P/V, respectively, without the addition of synthetic polymers and with the addition of PVA, PVP or P68. The final concentration of each other is 0.2 %P/V. The matrix was finally re-suspended in distilled water.

2.3. Matrixes characterization:

2.3.1. Scanning electron microscopy: SEM micrographs of the surface of the beads were performed using a scanning electron microscope FEI Quanta 650 FEG Environmental SEM with 5.00 kV voltage for secondary electron imaging. The macroparticles were previously lyophilizates.

2.3.2. Determination of pH_{ZPC}: pH at zero charge point (pHzpc) values for Alg-GG in the absence and presence of FCPs were determined in 0.1 N KCl at 20°C according to the method reported previously [14]. Sample (0.5 g) and 12.5 ml KCl 25mM were mixed in different reaction vessels. The pH of the suspension was then adjusted to

different initial pH values between 2 to 8, using either 0.1 N HCl or Na(OH) solutions. Each system was agitated in a shaker bath for 24 h. After settling, the final pH of each suspension was measured. The ΔpH (the difference between final and initial pH) values were then plotted against the initial pH values. The pH at which ΔpH is zero was taken to be the pH_{ZPC} [15].

2.3.3. Acid base titration of Alg-GG: 0.2 g of bed in 20 mL of water was titrated with increasing amount of HCl or NaOH 0.1 M with constant stirring, and then the pH was register. The amount of proton released or bound per unit of bed mass was calculated. The blank titrations (without the sample) were also carried out. The adsorbed amounts of H^+ or OH^- at the final pH were calculated from the amount of the HCl or NaOH added to the samples minus the amount of acid or base used by blank titration, the adsorption of H^+ or OH^- to the samples was plotted versus the final pH.

2.3.4. Swelling analysis: weighting an accurate mass of dried Alg-GG beads, they were immersed in 25 mM Citrate buffer at 20 ºC. At defined time intervals, the beads were withdrawn from the solution and the increase in the weight of the beads were measured as a function of time until constant mass. The swelling ratio (SR) was expressed as:

$$SR = \frac{w_2 - w_1}{w_1} \quad (1)$$

where w_1 and w_2 represent the dry and wet weight of the beads, respectively.

2.4. Adsorption experiments:

2.4.1. Batch adsorption experiments: All adsorption experiments were conducted in batch mode with stirring speed of 30 rpm. The mixtures were stirred until the adsorption equilibrium was reached and the free protein in the supernatant was determined. The amount of QTg adsorbed was calculated from mass balance. The data was processed as % protein adsorbed/g matrix or as mass of adsorbed QTg over mass unit of hydrated

matrix. All measures were carried out at 25ºC. The ratio Alg/GG mass was 0.6 %p/v/0.5%p/v according to previous studies [13].

2.4.2 Experimental statistical design: The experimental designs and calculation of the predict data were carried out with Minitab® 17.1.0 (©Minitab Inc., 2013). Several independent experiments were performed to obtain optimized models for QTg adsorption. The influence of the variables, pH and synthetics polymers addition, on adsorption capacity was studied employing a general full factorial design with these factors in four and three levels, respectively. These factors and levels were determined by preliminary tests and literature [13, 16, 17]. The statistical significance of the non-linear regression was determined by Student's test, the second order model equation was evaluated by Fischer's test and the proportion of variance explained by the model obtained was given by the coefficient of determination, R^2.

The optimal levels of the significant factor in the QTg adsorption were analyzed by Fibonacci sequence [18]. In this study, one factor (pH) was tested. The used strategy had a maximum error of 0.1 with a range of pH between 4 and 6.

2.4.3. Adsorption kinetics: batch adsorption experiments of commercial QTg onto cross-linked Alg-GG beads were carried out measuring the concentration of free QTg in the supernatant over time. To analyze the kinetic adsorption mechanism, the amount of QTg adsorbed over mass unit of matrix vs. time curves were fitted with two models, namely pseudo-first and pseudo-second order [19]. The mixtures were prepared with 25 mM citrate buffer at pH 5.0, 5.08 and 4.92 depending on the case, and stirring constantly at 30 rpm until the adsorption equilibrium was reached.

2.4.4. Adsorption isotherms: Adsorption isotherm of QTg was determined by equilibrating different concentrations of QTg with 100 mg cross-linked Alg-GG beads at pH 5.0, 5.08 and 4.92 depending on the case at 25 °C. The mixtures were stirred until the adsorption equilibrium was reached and free protein in the supernatant was determined. The amount of QTg adsorbed at equilibrium time by unit of mass adsorbent (m) was calculated by the following equation:

$$Q_{eq} = \frac{\mathrm{Vx}(C_{eq} - C_0)}{\mathrm{m}} \quad (2)$$

Where: Q_{eq} is the quantity of protein adsorbed per gram of adsorbent (mg/g), C_0 is the concentration of residual protein in solution (mg/mL) and C_{eq} is the concentration of residual protein in the supernatant at equilibrium (mg/mL), V is the volume of solution (mL) and m is the mass of adsorbent (g). The results were expressed as Q_{eq} vs. $C_{eq.}$ To estimate the validity of isotherm models with experimental data the Langmuir, Freundlich and Hill models were tested [20-22].

2.5. Data Analysis: Non-linear regression analysis was applied to estimate the parameters of the isotherm and kinetic model. It was performed using a trial and error method with the help of Sigma Plot v12 software. The parameters were estimated by maximizing the coefficient of determination R^2 (sum of squares) and minimizing the value of SS (least sum of squares). Both coefficients have been widely employed to measure the fitting degree of the model to the adsorption data [23].

3. Results

3.1. Physical characterization of the matrix:

3.1.1. pH_{ZPC} and acid base titration of Alg-GG: The pH_{ZPC} values of Alg-GG in the absence and presence of FCP are shown in Table I and figure 1. The observed values for the bed in presence of PVP was 5.80, while the presence of PVA shifted this value to 5.98 and the P68 addition increases the value a 6.47, which suggests a slightly decrease of the negatively groups in the bed surface due to the presence of the FCP [23]. The acid-base titration of the bed also showed a decrease in the pK_a value in presence of FCP in comparison to the Alg-GG alone, suggesting that the presence of the FCP modifies the micro dielectric constant environment of the negatively electrical charged groups (COO^-) increasing their acidity (Table I). This effect can be assigned to the different hydrophobicity-hydrophilicity balance of the FCP molecule assayed.

Table I: Characterization results for the Alg-GG matrixes.

System	pH_{zpc}	pKa	Water %
Alg-GG	5.80	5.53	97.2 ±0.1
Alg-GG- PVA	5.98	5.44	96.0 ±0.1
Alg- GG-PVP	5.84	5.38	94.8 ± 0.2
Alg-GG- P68	6.47	5.33	96.0 ±0.1

3.1.2. Swelling analysis: the swelling study of the beads was carried out at pH 5.0 using citrate buffer. A difference in the swelling process in absence and presence of FCP was observed, as shown in Table I. Blends of polysaccharides with synthetic polymers have been shown to have many applications, given the biocompatibility of many synthetic flexible chain polymers, such as ethylene-propylene oxides, etc. [23]. There is evidence that PVA, PVP and P68 tend to interact with the OH groups of polysaccharides,

forming Hydrogen Bridge, such as P68, where the -O-ether interacts through hydrogen bonds with OH polysaccharides [24, 25]. The strength of this interaction depends on the ability to form a hydrogen bond with the polysaccharide chain, in the following sense: PVP <P68 <PVA. A higher capacity to form a net, more rigid is the structure of the bed offering greater mechanical resistance. However, another important property is that the rigidity, which decreases the amount of water that the bed retains, inducing an increase in the uptake rate of QTg which increases the adsorption capacity of the bed per unit mass [23].

3.1.3. Scanning electron microscopy: The four obtained matrixes were lyophilized and then, morphologically studied by SEM. The images of them are shown in Figure 2. The morphological aspect of the Alg-GG surface changed substantially with the inclusion of FCP. According to SEM micrographs, the Alg-GG surface presents a little roughness that increase with the addition of FPC. However, the surface roughness of each FPC were different. The PVA and PVP addition, 2b and 2d, respectively, showed an increase in the quantity of pores presents in their surfaces. This phenomenon has also been seen for other polymeric systems [26]. On the other hand, the P68 addition showed a scaly surface with more porosity. It is believed that P68 interacts with alginate mostly through hydrophilic interactions, due to the high -OH content, which induces an extended conformation of the polymers in solution. Considering the hydrophilic/hydrophobic character of P68, it can be assumed that those molecules must be oriented with their polar chains interacting with water or with the polysaccharides, and with their non-polar chain interacting with the air trapped inside the pore. In this way, the presence of the surfactant molecules permits us to maintain the structural integrity of the membrane as water evaporates[27]. Results suggest that the addition of nonionic polymers produce surface changes on matrixes that can be affect adsorption capacity of the beds.

3.2. *Optimization of QTg adsorption onto ALG-GG matrixes*: The experimental design and results, according to the general full factorial design, are shown in Table II where the significance of pH and polymer type on QTg adsorption is shown.

Table II: Experimental design and results according to the general full factorial design.

Experiment	pH	FCP	Adsorption (%)
1	6	PVA	41.9
2	6	P68	34.8
3	7	PVP	16.2
4	4	P68	46.8
5	5	P68	60.9
6	4	PVA	46.3
7	4	PVP	35.7
8	7	PVA	17.6
9	6	PVP	37.3
10	5	PVA	48.7
11	5	PVP	60.7
12	7	P68	19.6
13	5	P68	71.8
14	5	PVP	63.2
15	5	PVA	56.2

The goal in applying this type of experiment is to obtain a model that selects the most important factor while investigating the interactions between all the levels of the categorical variables involved. Through the analysis of the variance, the statistical significance of each variable and their interactions were verified. In the analysis of the adsorption capacity, it was possible to verify that the interaction between polymer type and pH was not significant, proceeding to its removal from the analysis. The following equation (1) shows the influence of the variables assayed on the adsorption capacity of the bed:

$$\%_{Ads} = 38.88 + 4.06\ pH4 + 17.89\ pH5 - 0.88\ pH6 - 21.07\ pH7 + 1.65\ P68 - 1.40\ PVP - 0.25\ PVA \quad (3)$$

It was possible to conclude that the pH is the only significant variable influencing the adsorption capacity of the matrix ($P < 0.05$). R^2 indicates that the adjusted model explains 92.59% of the variability of this dependent variable. Thus, the response surface based on this model was used to represent the adsorption capacity as a function of independent variables as shown Figure 3.

Comparing the effect produced by the addition of the synthetics polymers was clearly insignificant in the adsorption capacity between each other. However, the change in pH caused an increase in the adsorption capacity of QTg, with a maximum pH value near 5.0. At higher pH levels, a decrease in the adsorption was observed. The explanation for this is that the Alg has carboxyl groups which dissociate at pH 4.5, while QTg has an isoelectric pH around 8.5. Consequently, at pH levels higher than 5 the positive electrical charge of the protein decreases, reducing the electrostatic interaction between the opposite electrical charges.

Through the Fibonacci sequence an optimization strategy for 1 factor and 1 response, unvaried problem, was developed, and considering the earlier results, successive pH values with a symmetrical difference between them where studied for the addition of these synthetic polymers (PVA, PVP and P68). The best QTg adsorption capacity for each polymer is pH 4.92 for Alg-GG-PVA matrix; pH 5.08 for Alg-GG-PVP and Alg-GG-P68 matrixes. The following experiments were carried out at each pH level, respectively.

3.3 Kinetics of the QTg adsorption onto de ALG-GG matrixes: Figure 4 shows the adsorption kinetic curves for QTg onto Alg/GG matrixes. It was observed that at approximately 40 min the curve reaches a plateau stage, which indicates that the

adsorption was a fast process. In addition, it was observed that the presence of FCP increases the adsorption capacity by mass unity of bed, showing that PVP and PVA have a major effect.

To obtain information about the adsorption mechanism of QTg onto the Alginate GG matrix, pseudo-first order and pseudo second order kinetic models were fitted to the experimental data. The kinetic model's constants, coefficients of determination and average relative error are shown in Table III. It was observed that the pseudo-first order model is the model that best fitted the data, the second order fitting model gives Qe values higher than those observed from visual inspection of the data in Figure 3, which suggests that the adsorption follows the pseudo-first order model. Also, the Qe value shows clearly that the presence of PVA and PVP increases the adsorption capacity of the bed in the order of 17 and 35 % respectively.

Table III: Kinetic parameters for the QTg adsorption on Alg-GG matrixes. 25 mM Citrate buffer pH 5.0, 5.08 and 4.92, as appropriate. [QTg] 0.164 mg / ml. Temperature 25ºC

Matrix	Model	Qe ($mg.g^{-1}$)	k1 (min^{-1})	k2 ($g.mg^{-1}.min^{-1}$)	R^2	SS
Alg-GG	Pseudo first Order	1.42±0.17	0.03±0.007		0.9676	0.0526
	Pseudo second Order	2.17±0.92		0.01±0.006	0.9678	0.0523
Alg-GG-P68	Pseudo first Order	1.44±0.14	0.06±0.01		0.9471	0.1092
	Pseudo second order	2.03±1.09		0.02±0.01	0.9503	0.1027
Alg-GG-PVA	Pseudo first order	1.67±0.04	0.09±0.008		0.9774	0.0843
	Pseudo second order	2.10±1.50		0.04±0.008	0.9769	0.0896
Alg-GG-PVP	Pseudo first order	1.92±0.30	0.05±0.02		0.9387	0.2179
	Pseudo second order	2.97±1.36		0.01±0.01	0.9346	0.2326

The dynamics of the adsorption mechanism can be described by the following consecutive steps [28]: transport of the solute from the bulk solution through the liquid film to the adsorbent surface; solute diffusion into the pore of the adsorbent; parallel to this occurs the intra-particle transport mechanism and; adsorption of the solute on the interior surfaces of the pores and capillary spaces of the adsorbent.

The third step is assumed to be rapid and considered to be negligible, so adsorption rate will be controlled by the slowest step, which would be either film or pore diffusion. The

most commonly used technique for identifying the mechanism involved in the adsorption processes is by fitting the experimental data in an intra-particle diffusion plot. Previous studies [28, 29] showed that a plot of Qe vs. $t^{0.5}$ represents multi-linearity, which characterizes the two or more steps involved in a adsorption process. The intra-particle diffusion model is given in a simplified form by [29] :

$$Qe = K_{id} t^{0.5} + C \qquad (4)$$

where K_{id} is the intra-particle diffusion coefficient (mg/g $min^{0.5}$) and C is a constant related to the extent of the boundary layer effect. Thus, the K_{id} (mg/g $min^{0.5}$) value can be obtained from the slope of the plot of Qe (mg/g) versus $t^{0.5}$ ($min^{0.5}$) as shown in Figure 5. The slope of the straight line has been defined as the intra-particle diffusion parameter K_{id} (mg/g $min^{0.5}$), (according to equation 2). The presence of FCP increases the K_i value, which is related to the increase in the diffusion process of QT_g in the following order: none (0.1815 ± 0.0108) < P68 (0.2309 ± 0.0169) < PVA (0.2557 ± 0.0189) < PVP (0.3185 ± 0.0323). The linear relationship showed in Figure 5, suggests that the only process which controls the total adsorption process of QT_g is the pore diffusion. The straight lines obtained in Fig. 5 passes approximately through the origin, indicating that pore diffusion is the main rate-limiting step [30]. Studies about the dyes adsorption onto more complex matrix such as biomass yielded a plot which can be represented by three lines, indicating that the adsorption rate is controlled by three adsorption stages. According to reference [31], the first line at the beginning of the adsorption process represents the external mass transfer with a high adsorption rate while the second line indicates the intra-particle diffusion. In our case the first phase of adsorption, the high rate stage, could not be detected while only the second phase of intra particle diffusion is observed in the data from Fig. 5. So, the presence of FCP

induce an increase in the kinetics of this process due to an increase in the hydration of the pore walls, decreasing the interaction with the macromolecule.

3.4. Adsorption isotherm of QTg onto Alg-GG in the absence and presence of FCP: Figure 6 shows the QTg adsorption isotherms onto Alg-GG bed and the effect of the presence of three different FCP used to obtain the beds. The isotherm parameters were obtained fitting the data using two isotherms models: Freundlich and Langmuir. Table IV resumes the values obtained. All the systems (in absence and presence of FCP) showed to follow a Freundlich behavior, this model showed to best fit the data.

.

Table IV: Parameters of the QTg adsorption process on Alg-GG matrixes. Medium Buffer 25 mM Citrate at pH 5.0, 4.92 or 5.08, as appropriate. Temperature 25ºC.

Matrix	Model	K_F	K_L	n_F	Q_0 (mg.g^{-1})	R^2	SS
	Freundlich	15.3 ± 2.7		0.89 ± 0.09		0.9673	0.2783
Alg/GG	**Langmuir**		(-)0.6±0.5		(-)17.9±1.3	0.9646	0.3013
	Freundlich	15.9±1.24		1.04±0.04		0.9912	0.1212
Alg/GG/P68	**Langmuir**		0.28±0.34		65.2±1.04	0.9909	0.1256
	Freundlich	17.9±1.2		1.01±0.04		0.9954	0.0761
Alg/GG/PVA	**Langmuir**		0.09±0.29		208.8±0.92	0.9955	0.0754
	Freundlich	18.6±3.3		0.96±0.09		0.9723	0.4453
Alg/GG/PVP	**Langmuir**		(-)0.32±0.63		(-)51.4±2.01	0.9725	0.4415

According to the Freundlich equation:

$$q_e = K_F C_e^{1/n_F} (5)$$

where q_e denotes the adsorbate adsorbed per gram of adsorbent at the equilibrium, *Ce* is the equilibrium concentration of adsorbate in liquid phase, K_F, n_F are empirical constants that indicate the extent of adsorption and the adsorption effectiveness, respectively, n_F in the case of Freunlich isotherm depends on the adsorbent and the adsorbate type, in this case, because the adsorbate is the same (QTg), the difference in the n_F values will be due to the adsorbent (in presence or not of FCP). From Table IV, the presence of FCP induced an increase in the K_F value following the order: none < P68 < PVA < PVP, suggesting an increase in the adsorption capacity of the bed in correlation with the behaviour observed in the adsorption kinetics of QTg. The conclusion is that the FCP addition not only facilitates the adsorption process, it also increases the bed capacity. The analysis of the n_F values was inconclusive because it's value did not show any variation with the presence of the FCP.

The adsorption showed to be reversible, by increasing the ionic strength of the medium in the systems Alg-GG, Alg-GG-PVP and Alg-GG-PVA. These matrixes were chosen for the study of desorption since in the adsorption study they were responsible for obtaining the highest amount of QTg adsorbed per g of matrix. The NaCl addition in the citrate buffer used, showed the elution of the QTg adsorbed onto the bed. The presence of FCP modifies the capacity of adsorption and desorption of the bed as is illustrated in table V.

Table V: Mean of eight QTg adsorption-washing-desorption cycles onto Alg-GG matrixes. Medium Buffer 25 mM Citrate at pH 5.0, 5.08 or 4.92 with 50 mM or 300 mM NaCl, as appropriate. Temperature 25ºC.

Matrix	Adsorption (%)	Desorption (%)
Alg-GG	37	96
Alg-GG-PVP	43	90
Alg-GG-PVA	48	100

PVA induced an increase in the adsorption of the protein by the bed and an increase in the desorption capacity.

It has been demonstrated that when PVA is incorporated in a Alg matrix hydrogel a semi-interpenetrating polymer network is formed [32] due to the formation of hydrogen bonds between the molecular chains of the polymers, this situation is poorly produced in the presence of PVP and null in the presence of P68 because of its incapacity to form hydrogen bonds.

4. Conclusion

Cross-linked Alg-GG matrixes have high water content, so they are a mild environment for proteins, increasing their stability. To assess the matrixes structure, some physicals features studies were carried out, like pHzpc, acid basic titration and SEM. A swelling study reveals high degree of swelling of the prepared beds due to the high content of hydrophilic groups. It was also observed that cross-linking of Alg-GG/FCP beads did not reduce the swelling behavior in a significant manner and enhanced the hydrophilicity, as is demonstrated by increasing the diffusion constant of the adsorption process. The SEM images indicated that the FCP addition changes bed surface and morphology.

The adsorption kinetic data shows to follow a pseudo-first order kinetic model for all the beds assayed, because this fitting model provides better correlation with the experimental data at different initial concentrations of adsorbate. Freundlich isotherm describes the heterogeneous system and reversible adsorption and it's not restricted to the monolayer formation. This model predicts that the protein concentration in the adsorbent increases with the increase in its initial concentration in solution. While the adsorption process showed to be reversible because the QTg was released from the bed using a low concentration of NaCl, also this is a proof of the electrostatic nature of the interaction. The optimal adsorption pH was around 5.00, which correlates with the isoelectric point of the QTg around of 8.5, the increase of pH to higher values results in a decrease in the adsorption due to the loss of positive electrical charge of the protein. The obtained Alg-GG matrixes with PVA or PVP addition have shown to be efficient in the QTg adsorption. This is an important result, because this system should be used as a first step in the recovery of QTg from fresh pancreas homogenate. Furthermore, the low-cost technique and the biomaterials used guarantee the inexpensive, non-hazardous, and environmentally benign process.

Acknowledgements

This research was supported by grants from FonCyT, Projects PICT 2013 - 271-Argentina Innovator 2020. M.E Brassesco thank FonCyT and N. Woitovich Valetti Thank CONICET for their fellowship. We thank Paola Camiscia for the language correction of the manuscript.

Figures Legends:

Figure 1: pH_{ZPC} of the Alg-GG matrixes at 25ºC.

Figure 2: SEM micrographs of beads obtained with: a) Alg-GG b) Alg-GG-PVA c) Alg-GG-P68 d) Alg-GG-PVP.

Figure 3: Response surfaces QTg adsorption capacity by Alg-GG matrix.

Figure 4: Kinetics curves in the optimal conditions for the adsorption of QTg (initial concentration 0.164 mg/ml), pH 5.00, 5.08 and 4.92 depending on the case at 25 °C.

Figure 5: Weber–Morris kinetic plots for the QTg adsorption onto Alg-GG bed in the absence and presence of FCP. All data were taken from Figure 4.

Figure 6: Adsorption isotherms of QTg onto Alg-GG beds. Medium: 25 mM Citrate buffer pH 5.00, 5.08 and 4.92 depending on the case. Temperature: 25 °C

5. References

1. Blow, D.M., *Structure and mechanism of chymotrypsin.* Accounts of chemical research, 1976. **9**(4): p. 145-152.
2. Kunitz, M. and J.H. Northrop, *Crystalline chymo-trypsin and chymo-trypsinogen.* I. Isolation, crystallization, and general properties of a new proteolytic enzyme and its precursor, 1935. **18**(4): p. 433-458.
3. Kunitz, M. and J.H. Northrop, *Isolation from beef pancreas of crystalline trypsinogen, trypsin, a trypsin inhibitor, and an inhibitor-trypsin compound.* The Journal of general physiology, 1936. **19**(6): p. 991-1007.
4. Guyonnet, V., et al., *Purification and partial characterization of the pancreatic proteolytic enzymes trypsin, chymotrypsin and elastase from the chicken.* Journal of Chromatography A, 1999. **852**(1): p. 217-225.
5. Valetti, N.W., et al., *Precipitation of chymotrypsin from fresh bovine pancreas using ι-carrageenan.* Process biochemistry, 2012. **47**(12): p. 2570-2574.
6. Braia, M., et al., *Complex formation between protein and poly vinyl sulfonate as a strategy of proteins isolation.* Journal of Chromatography B, 2008. **873**(2): p. 139-143.
7. Alvarez-Lorenzo, C., et al., *Crosslinked ionic polysaccharides for stimuli-sensitive drug delivery.* Advanced drug delivery reviews, 2013. **65**(9): p. 1148-1171.

8. Ngah, W.W., C. Endud, and R. Mayanar, *Removal of copper (II) ions from aqueous solution onto chitosan and cross-linked chitosan beads.* Reactive and Functional Polymers, 2002. **50**(2): p. 181-190.

9. Piyakulawat, P., et al., *Preparation and evaluation of chitosan/carrageenan beads for controlled release of sodium diclofenac.* Aaps PharmSciTech, 2007. **8**(4): p. 120-130.

10. Vennapusa, R.R., et al., *Biomass-adsorbent adhesion forces as an useful indicator of performance in expanded beds.* Separation Science and Technology, 2010. **45**(15): p. 2235-2244.

11. Vennapusa, R.R. and M. Fernandez-Lahore, *Effect of chemical additives on biomass deposition onto beaded adsorbents.* Journal of bioscience and bioengineering, 2010. **110**(5): p. 564-571.

12. Roy, I., M. Sardar, and M.N. Gupta, *Cross-linked alginate–guar gum beads as fluidized bed affinity media for purification of jacalin.* Biochemical engineering journal, 2005. **23**(3): p. 193-198.

13. Brassesco, M.E., N.W. Valetti, and G. Picó, *Molecular mechanism of lysozyme adsorption onto chemically modified alginate guar gum matrix.* International journal of biological macromolecules, 2017. **96**: p. 111-117.

14. Tan, W.-f., et al., *Determination of the point-of-zero charge of manganese oxides with different methods including an improved salt titration method.* Soil Science, 2008. **173**(4): p. 277-286.

15. Salis, A., et al., *Measurements and theoretical interpretation of points of zero charge/potential of BSA protein.* Langmuir, 2011. **27**(18): p. 11597-11604.

16. Dotto, G., et al., *Optimization and kinetic analysis of food dyes biosorption by Spirulina platensis.* Colloids and Surfaces B: Biointerfaces, 2012. **91**: p. 234-241.

17. Valetti, N.W. and G. Picó, *Adsorption isotherms, kinetics and thermodynamic studies towards understanding the interaction between cross-linked alginate-guar gum matrix and chymotrypsin.* Journal of Chromatography B, 2016. **1012**: p. 204-210.

18. Massart, D.L., et al., *Handbook of chemometrics and qualimetrics: Part A.* 1997: Elsevier Science Inc.

19. Kumar, M., R. Tamilarasan, and V. Sivakumar, *Adsorption of Victoria blue by carbon/Ba/alginate beads: Kinetics, thermodynamics and isotherm studies.* Carbohydrate polymers, 2013. **98**(1): p. 505-513.

20. Foo, K. and B. Hameed, *Insights into the modeling of adsorption isotherm systems.* Chemical Engineering Journal, 2010. **156**(1): p. 2-10.

21. Guerrero-Coronilla, I., L. Morales-Barrera, and E. Cristiani-Urbina, *Kinetic, isotherm and thermodynamic studies of amaranth dye biosorption from aqueous solution onto water hyacinth leaves.* Journal of environmental management, 2015. **152**: p. 99-108.

22. Rangabhashiyam, S., et al., *Relevance of isotherm models in biosorption of pollutants by agricultural byproducts.* Journal of Environmental Chemical Engineering, 2014. **2**(1): p. 398-414.

23. Doğan, M., Y. Özdemir, and M. Alkan, *Adsorption kinetics and mechanism of cationic methyl violet and methylene blue dyes onto sepiolite.* Dyes and Pigments, 2007. **75**(3): p. 701-713.

24. Hua, S., et al., *pH-sensitive sodium alginate/poly (vinyl alcohol) hydrogel beads prepared by combined Ca 2+ crosslinking and freeze-thawing cycles for controlled release of diclofenac sodium.* International journal of biological macromolecules, 2010. **46**(5): p. 517-523.

25. Zain, N.A.M., M.S. Suhaimi, and A. Idris, *Development and modification of PVA–alginate as a suitable immobilization matrix.* Process Biochemistry, 2011. **46**(11): p. 2122-2129.

26. Kamoun, E.A., et al., *Poly (vinyl alcohol)-alginate physically crosslinked hydrogel membranes for wound dressing applications: characterization and bio-evaluation.* Arabian Journal of Chemistry, 2015. **8**(1): p. 38-47.

27. Bueno, C.Z., et al., *Control of the properties of porous chitosan–alginate membranes through the addition of different proportions of Pluronic F68.* Materials Science and Engineering: C, 2014. **44**: p. 117-125.

28. Vadivelan, V. and K.V. Kumar, *Equilibrium, kinetics, mechanism, and process design for the sorption of methylene blue onto rice husk.* Journal of colloid and interface science, 2005. **286**(1): p. 90-100.

29. Kousha, M., et al., *Box–Behnken design optimization of Acid Black 1 dye biosorption by different brown macroalgae.* Chemical Engineering Journal, 2012. **179**(Supplement C): p. 158-168.

30. Demiral, H., et al., *Adsorption of textile dye onto activated carbon prepared from industrial waste by ZnCl2 activation.* J. Int. Environm. Appl. Sci, 2008. **3**(3): p. 381-389.

31. Toor, M. and B. Jin, *Adsorption characteristics, isotherm, kinetics, and diffusion of modified natural bentonite for removing diazo dye.* Chemical Engineering Journal, 2012. **187**: p. 79-88.

32. Safi, S., et al., *Study of electrospinning of sodium alginate, blended solutions of sodium alginate/poly (vinyl alcohol) and sodium alginate/poly (ethylene oxide).* Journal of applied polymer science, 2007. **104**(5): p. 3245-3255.

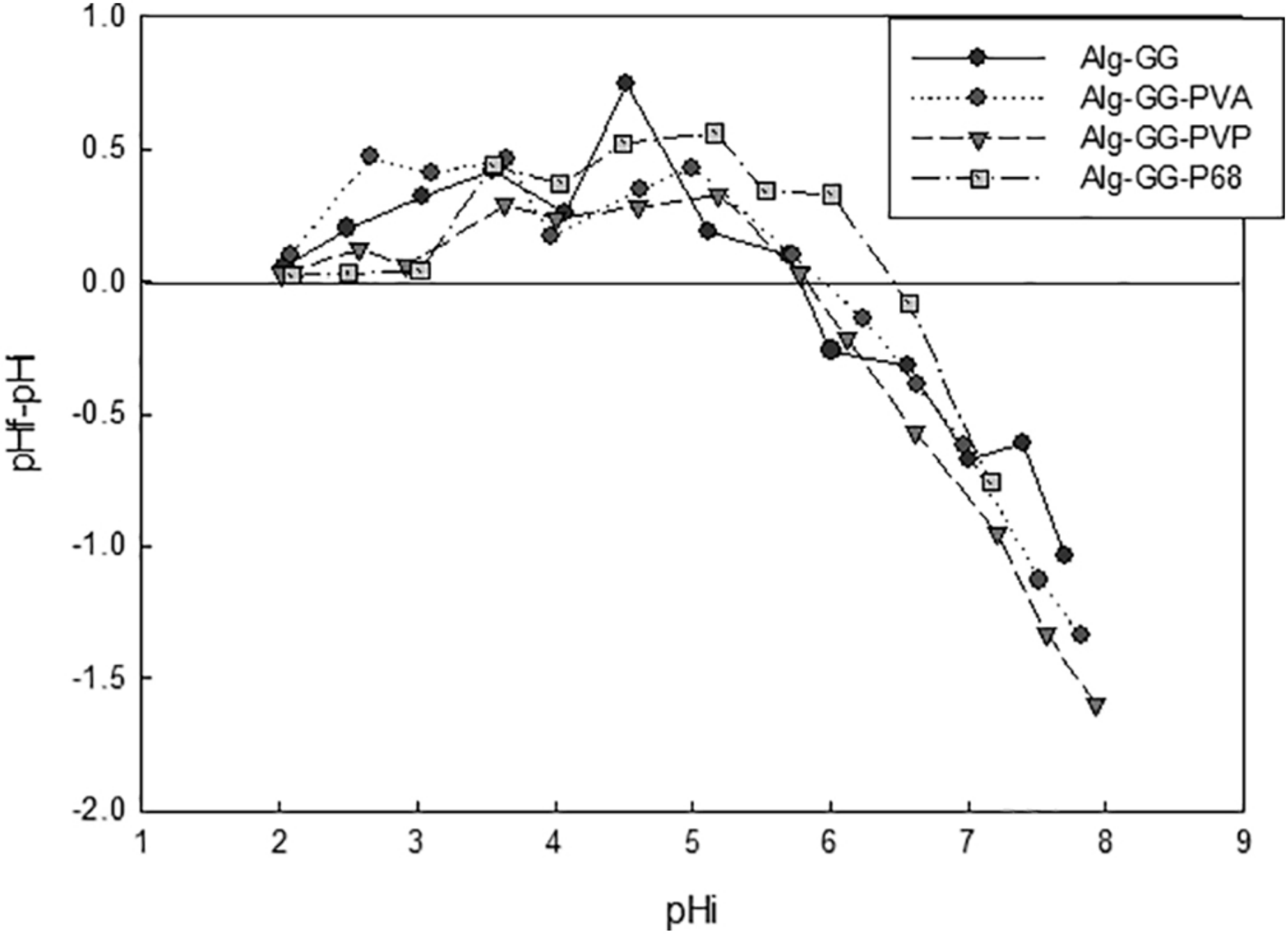
Alg-GG
Alg-GG-PVA
Alg-GG-PVP
Alg-GG-P68
pHf-pH
pHi
1.0
0.5
0.0
-0.5
-1.0
-1.5
-2.0
1
2
3
4
5
6
7
8
9

Figure 1

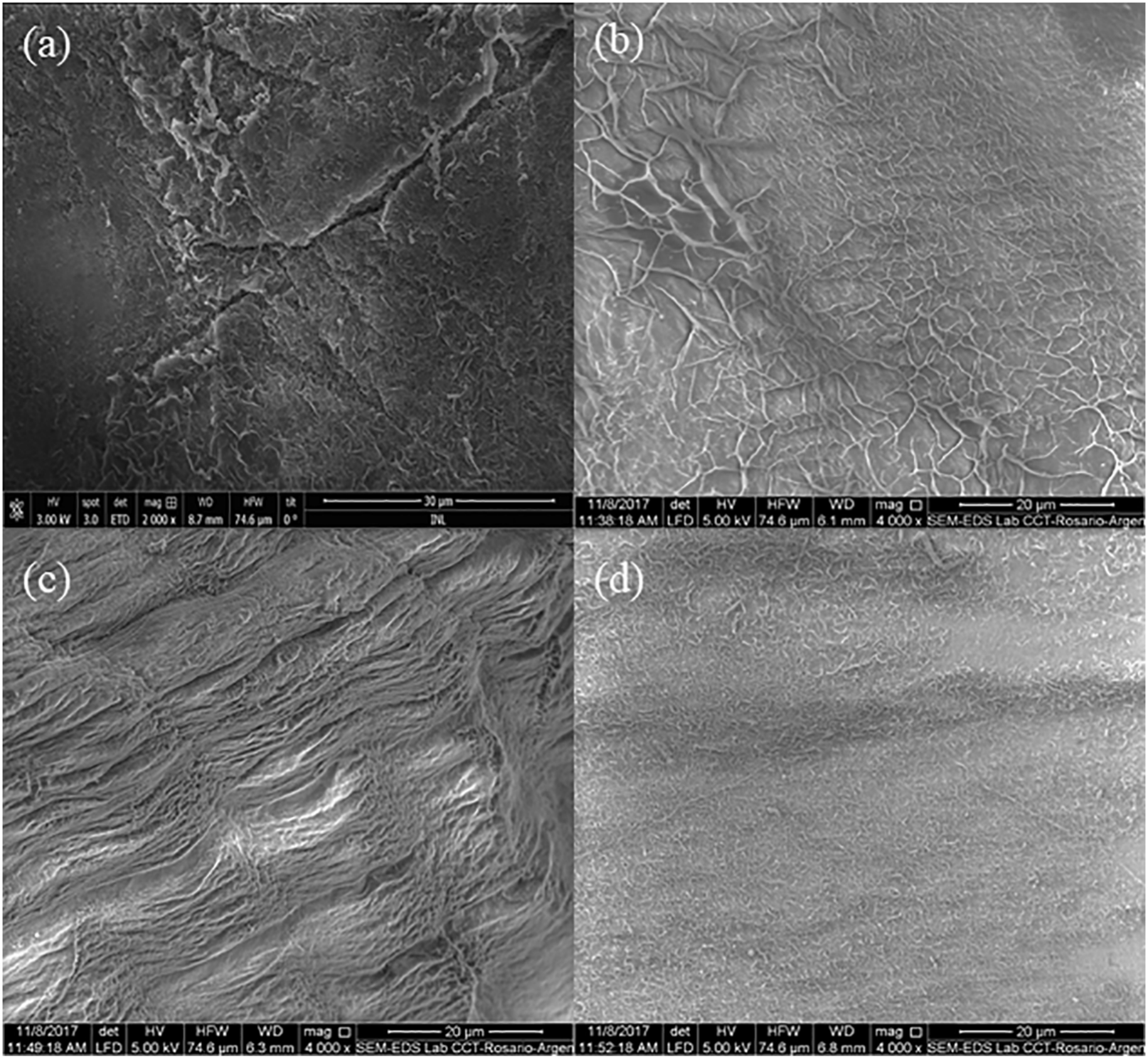
(a)
HV spot det mag WD HFW tilt
3.00 kV 3.0 ETD 2 000 x 8.7 mm 74.6 µm 0 °
30 µm
INL
(b)
11/8/2017 det HV HFW WD mag
11:38:18 AM LFD 5.00 kV 74.6 µm 6.1 mm 4 000 x
20 µm
SEM-EDS Lab CCT-Rosario-Argen
(c)
11/8/2017 det HV HFW WD mag
11:49:18 AM LFD 5.00 kV 74.6 µm 6.3 mm 4 000 x
20 µm
SEM-EDS Lab CCT-Rosario-Argen
(d)
11/8/2017 det HV HFW WD mag
11:52:18 AM LFD 5.00 kV 74.6 µm 6.8 mm 4 000 x
20 µm
SEM-EDS Lab CCT-Rosario-Argen

Figure 2

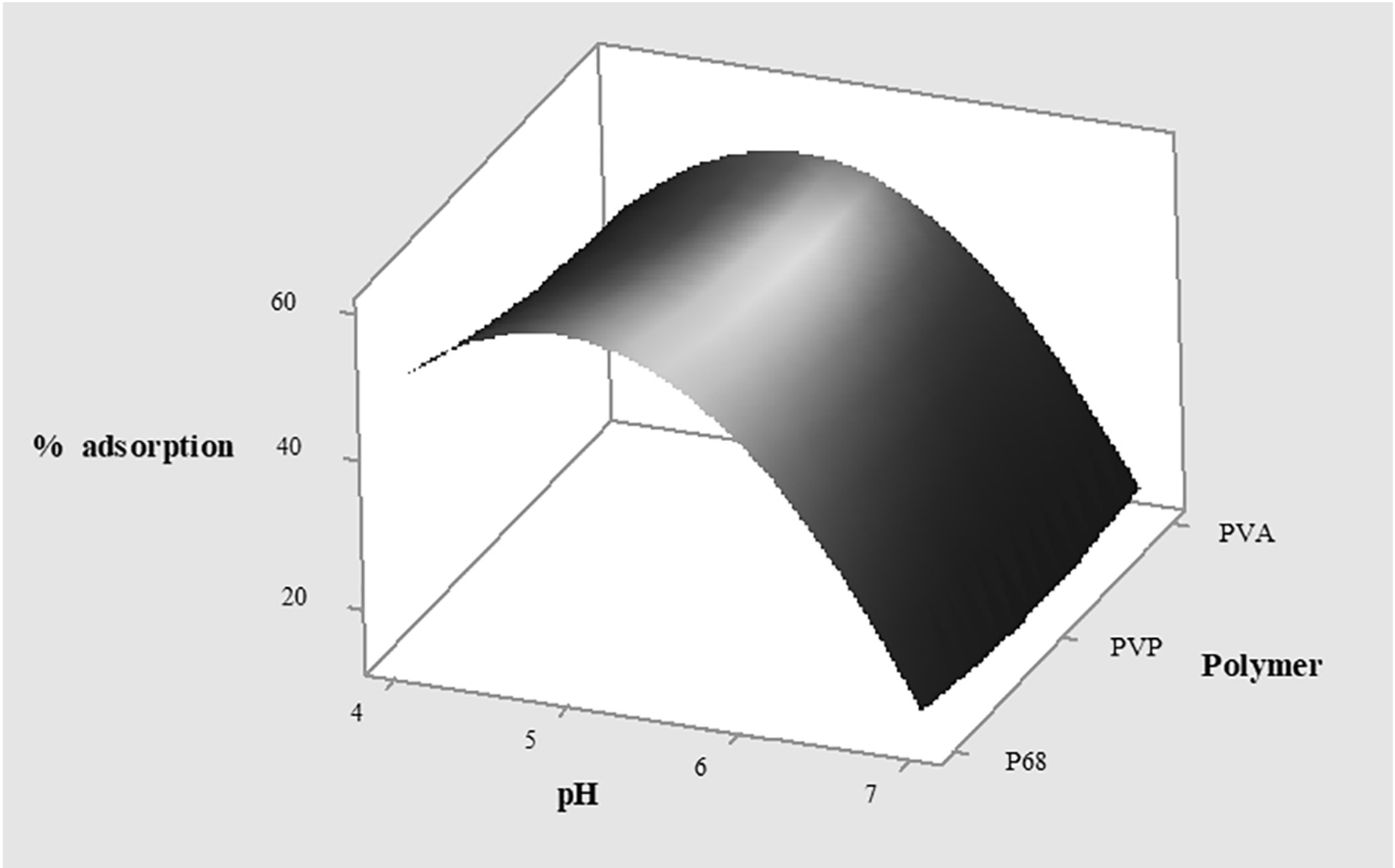

Figure 3

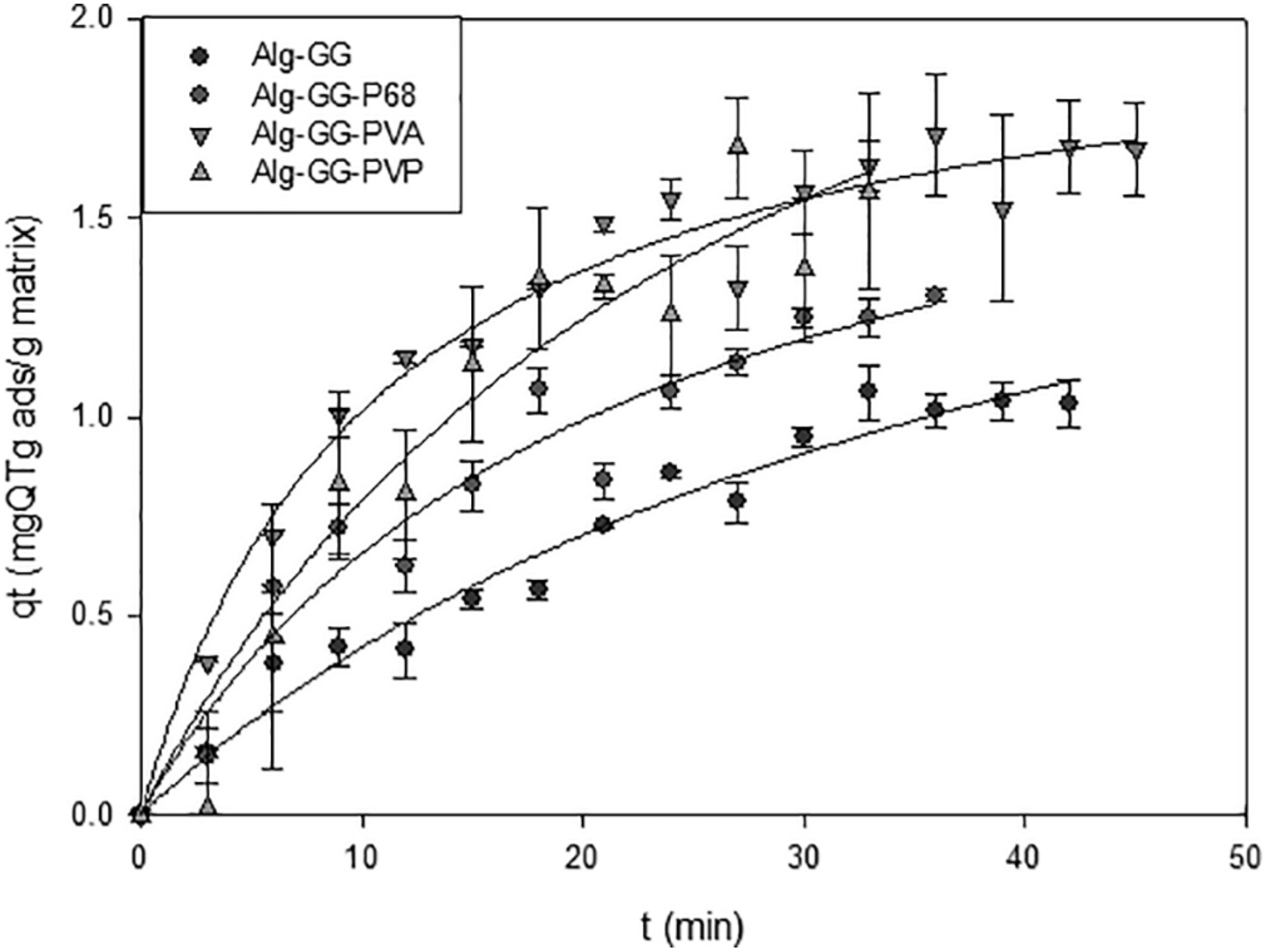
Alg-GG
Alg-GG-P68
Alg-GG-PVA
Alg-GG-PVP
qt (mgQTg ads/g matrix)
t (min)
0.0
0.5
1.0
1.5
2.0
0
10
20
30
40
50

Figure 4

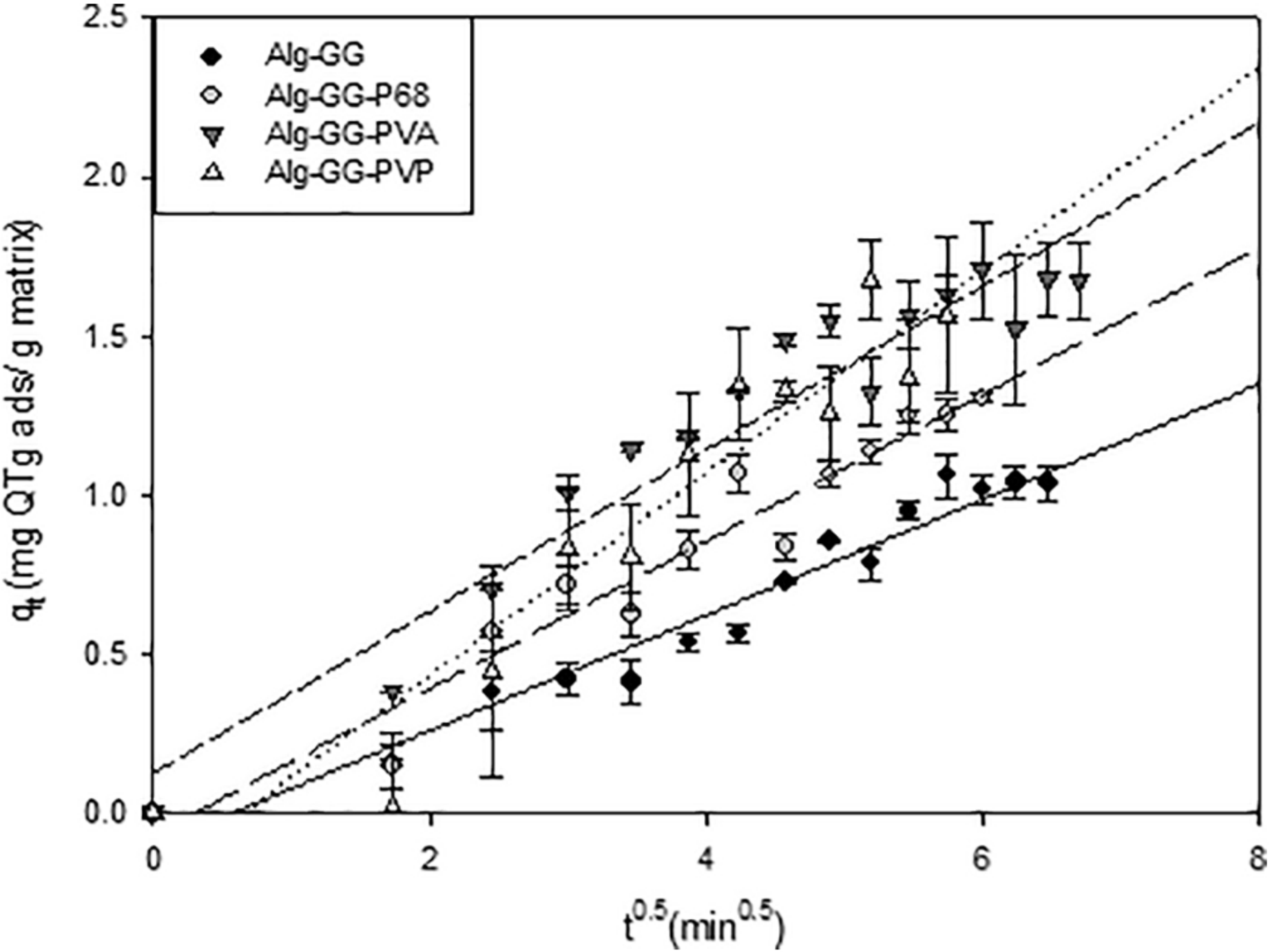
Alg-GG
Alg-GG-P68
Alg-GG-PVA
Alg-GG-PVP
q_t (mg QTg ads/ g matrix)
$t^{0.5}$(min$^{0.5}$)
0.0
0.5
1.0
1.5
2.0
2.5
0
2
4
6
8

Figure 5

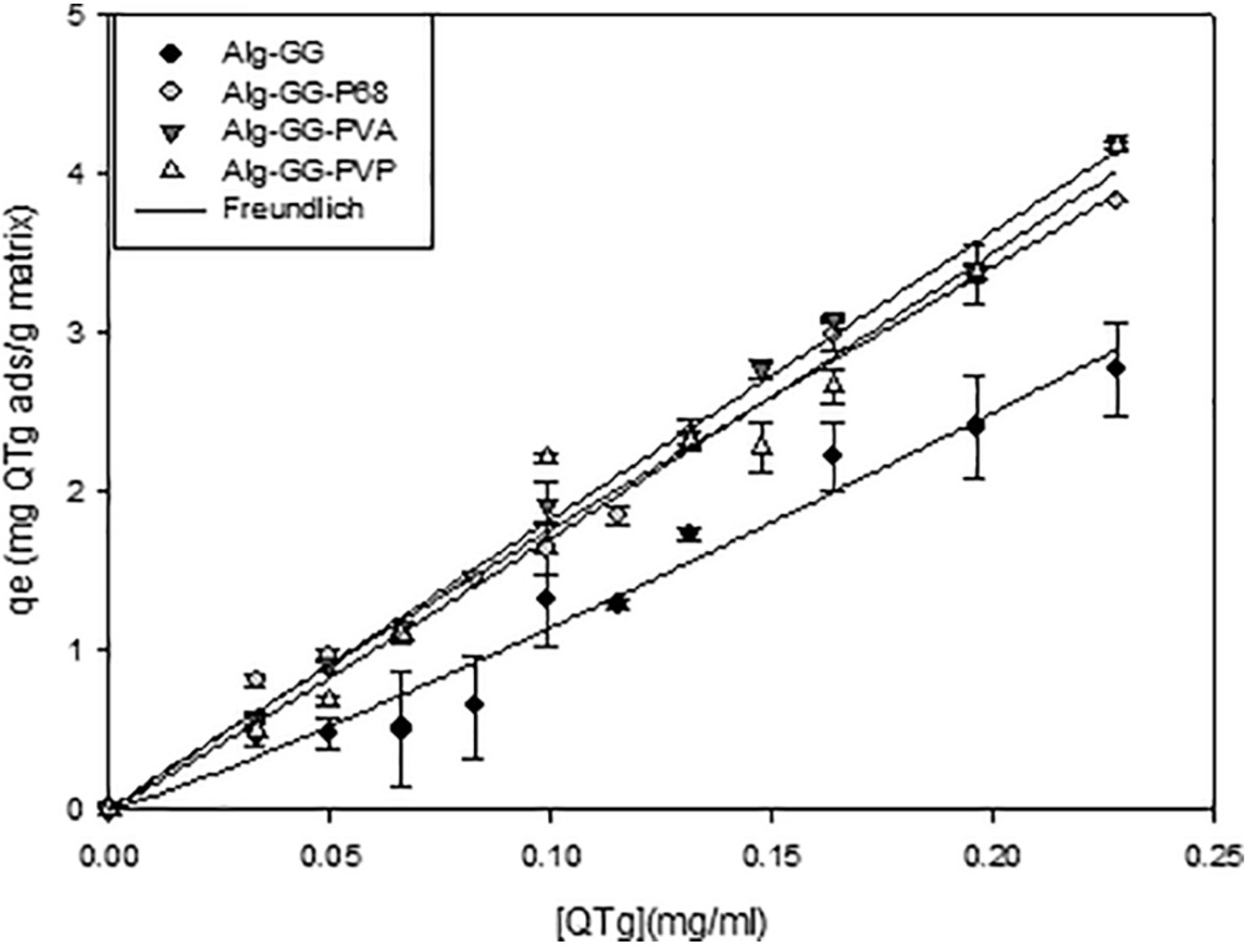
Alg-GG
Alg-GG-P68
Alg-GG-PVA
Alg-GG-PVP
Freundlich
qe (mg QTg ads/g matrix)
[QTg](mg/ml)
0
1
2
3
4
5
0.00
0.05
0.10
0.15
0.20
0.25

Figure 6